UCRL-96553
PREPRINT

Why Linear Birch and U_s-U_p Expansions Work

Richard Grover

This paper was prepared for submittal to
Proceedings of APS Topical Conference
on Shock Waves in Condensed Matter
Monterey, California
July 20-23, 1987

July 1987

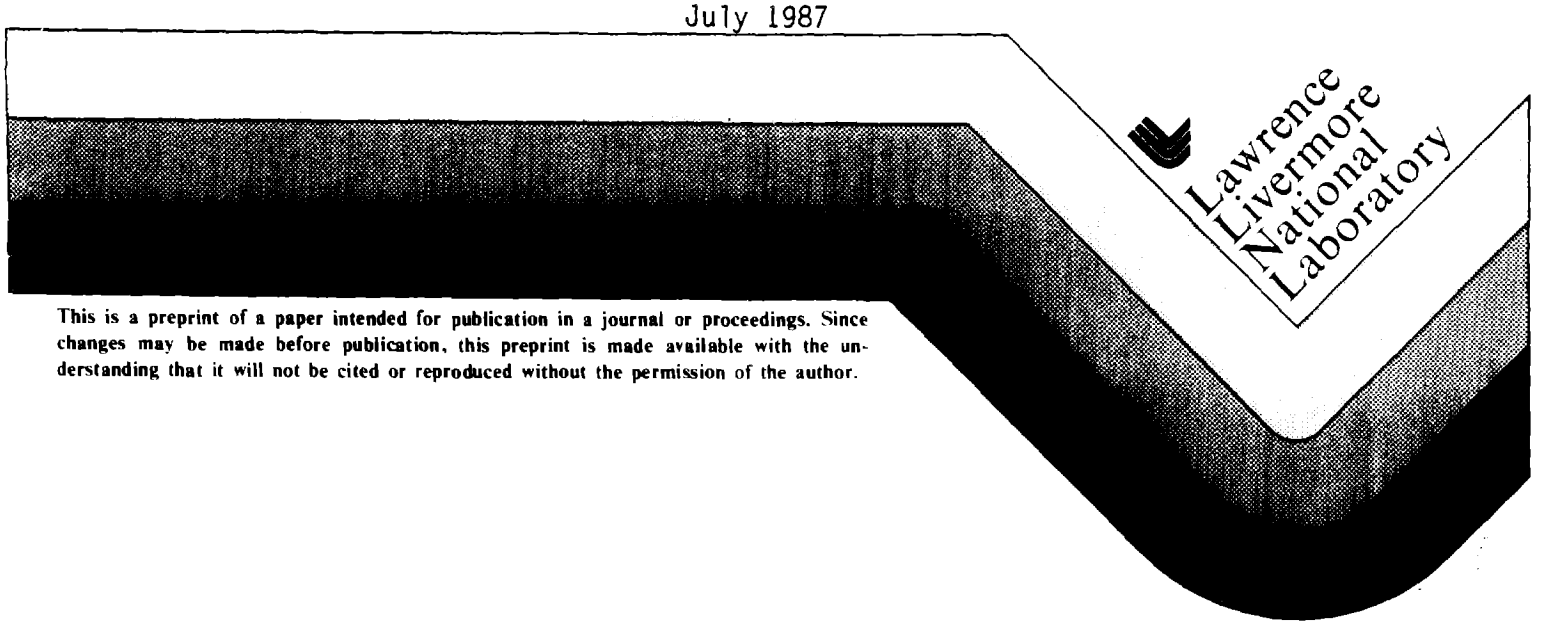

WHY LINEAR BIRCH AND U_S-U_p EXPANSIONS WORK

R. GROVER

Physics Department, University of California, Lawrence Livermore National Laboratory, P.O. Box 808, Livermore, California 94550*

The equivalence of the Birch-Murnoghan equation to a linear U_S-U_p equation was illustrated in the previous paper. Here we show in a direct manner how the virial theorem boundary localization of valence electron kinetic energy changes lead to the convergence of the Eulerian strain expansion about the zero-pressure state.

1. INTRODUCTION

As in the case of the velocity expansion of shock compression data, the Eulerian finite strain expression for isothermal pressure-density data on solids appears to converge so well that even in the best circumstances it shows little or no evidence for quadratic strain terms.[1,2] Since it is both systematic and convergent, the Eulerian strain expansion seems, therefore, to represent an optimum way of characterizing the static lattice equation of state of all types of solids over extended ranges of compression. However, a general physical explanation of this situation has unfortunately not been reported, although the consistency of shock compression data with standard, phenomenological pseudo-potential and pair-potential models has previously been discussed.[3]

Here we present a semiquantitative explanation of the convergence of the Eulerian strain expansion from the self-consistent electron band theory of solids in the local density approximation for exchange and correlation. This theory has provided a basis 9or nearly exact calculations of equation of state properties for a great variety of solids. Several static lattice calculations for simpler metals have in fact found to be well represented by nearly linear strain expansions out to compressions of 3. We find that the virial theorem can be used with this theory to relate the bulk modulus and its higher derivatives to electron kinetic energy changes during compression. McMahan[4] has already identified the latter as an important factor in changes of phase and electron bonding at high pressure. The necessary kinetic energy properties for convergence are then derived in a semiquantitative way from several appropriate models.

2. VIRIAL THEOREM APPLICATION TO BIRCH EQUATION

The virial theorem for Coulombic systems relates the kinetic energy t and potential energy Φ components of the internal energy E to the pressure P

$$E = t + \Phi \tag{1}$$

$$VP \equiv dE/d\ln\rho = \frac{2t}{3} + \frac{\Phi}{3} \tag{2}$$

If we separate first order energy changes into scaling, σ, and distortion, γ, components such as

* Work performed under the auspices of the U.S. Department of Energy by Lawrence Livermore National Laboratory under Contract W-7405-ENG-48.

$$dt = d_\sigma t + d_\gamma t \qquad (3)$$

then in Hartree-Fock theory $d_\gamma\phi = -d_\gamma t$ so that $d_\sigma E = 0$. In taking higher derivatives of Eq. (2) to study higher compression module the same cancellation is not complete and more complicated expressions result.

It is known that additional small terms must be added to the pressure Eq. (2) in the local density approximation. A rough estimate of the correction for the Hedin-Lundquist model for exchange-correlation is $\lesssim$ 20% the correlation energy. Looking ahead we will find that the desired properties depend on changes in the much larger, electron kinetic energies, permitting us to drop this and other correlation corrections from further consideration.

Thus we estimate bulk moduli and their high pressure derivatives from differentiations of (2) with respect to density, replacing ϕ by E-t and $dE/d\ell n\rho$ by P to get equation in terms electron kinetic energies and P. For instance the bulk modulus K and its first pressure derivative K', the Murnaghan parameter, are then given at zero pressure simply by

$$3V\,K_0 = dt/d\ell n\rho \equiv t' \qquad (4)$$

$$K_0' - 7/3 = d\ell nt'/d\ell n\rho \equiv \tau \qquad (5)$$

in terms of two convenient kinetic energy parameters t' and τ.

The linear Birch-Murnaghan equation of state is completely determined by these quantities, the pressure being scaled to K_0 and the coefficient of the linear strain term, A_1 by K_0'

$$A_1 = 3/2\,(K_0' - 4) \qquad (6)$$

The convergence of the strain expansion in the range of presently available compression data is then adequately evaluated by looking at the next two higher strain coefficients A_2 and A_3 which involve the next two pressure derivatives of K_0. By differentiating (2) twice more and with the use of (4) and (5) we may write these pressure derivatives at zero pressure in dimensionless form as

$$K_0K_0'' = -K_0' + \mathcal{O}\left(1 - \frac{\tau}{3} + d\tau/d\ell n\rho\right) \qquad (7)$$

$$K_0^2K_0''' = -2K_0'K_0K_0'' + \mathcal{O}\left[\left(\tau - \frac{1}{3}\right)d\tau/d\ell n\rho + d^2\tau/d(\ell n\rho)^2\right]. \qquad (8)$$

Empirically the K_0' is a large number in the range 3.5-6 for all solids of interest. The virial theorem then allows this to be done with smaller values of τ in the range 1-3, according to (5), which values we justify in the next section in terms of the behavior of electron kinetic energy in compression. Here we argue, mainly because of the large size of K_0', that the last terms in (7) and (8) are relatively small as indicated by the nomenclature. Dropping them, we may show the smallness of A_2 and A_3, which we express in the form

$$A_2 = \frac{3}{2}\left[K_0K_0'' + K_0' + \left(K_0' - \frac{11}{3}\right)\left(K_0' - \frac{13}{3}\right)\right] \qquad (9)$$

$$A_3 = \frac{9}{8}\left\{K_0^2K_0''' + 4K_0K_0''\left(K_0' - \frac{16}{3}\right) + \left[\left(K_0 - \frac{8}{3}\right)^2 + 6\right]\right\} \qquad (10)$$

Calculations of A_2 and A_3 in the indicated approximations (7) and (8) are shown in Table 1 to demonstrate their smallness.

Table 1

K_0'	3.5	4	5	5.5
A_2	.21	-.17	1.33	3.21
A_3	0.63	0.33	-0.54	0.57

Together with smallness of the Eulerian strain variable ($\sim \Delta R/R$) in the range of compression data ($< .5$) these assure very small non-linear strain contributions to the equation of state.[2]

3. MODEL CALCULATIONS OF τ

Here we can only qualitatively describe and summarize calculations of electron energy changes during compression. For this purpose it is useful to separate these changes into their scaling and distortional components; i.e. from (4)

$$t' = t'_\gamma + t'_\sigma \equiv \frac{d_\gamma t}{d\ell n\rho} + \frac{d_\sigma t}{d\ell n\rho} \qquad (11)$$

For example in the high density, uniform electron gas limit $t' \to t_\sigma' \simeq 2t/3$ and $\tau \to 2/3$.

At much lower densities contributions to kinetic energy changes, t', become increasingly localized the outer, more polarizable layers of the atom, as the higher energy valance electrons gradually become excluded from a rigid ion core. Such properties are readily seen in the electronic charge or potential distribution given by a Thomas-Fermi (TF) model, which model provides a realistic average model for equation of state. Table 2 presents some direct calculations of the kinetic parameter τ, (5), with the TF model over a wide range of interatomic radii (Z scaled).

Table 2. Kinetic energy parameter in Thomas-Fermi theory

$Z^{1/3}R$	∞	100	25	10	5	0
τ_{TF}	? $\leftarrow$	.45	.57	.65	1.0 $\to$ 2/3	

Thus in a TF gas model of compressibilities at normal densities, ranging over $2 < Z^{1/3}R_0 < 20$ from metallic H to C_s, kinetic energy changes raise values of K_0 to about 2/3 of normal values and because of the slow variation of τ with density are also consistent with the higher order approximations in Eqs. (7) & (8).

Boundary localization effects play an even stronger role in full electron-band theory calculations of energy changes around normal solid densities. Here electrons find themselves in band states of definite angular momentum ℓ (approximately) which are confined to a region outside of a fixed ion core, increasing the sensitivity of their kinetic energy to compression of the atomic cell. Volume independent core exclusion can arise both from the centrifugal potential in non-zero ℓ states and from orthogonalization to much lower states of the same ℓ in non-threshold cases. These features are indeed built into the concept of electron pseudo-potentials and can be treated in a perturbation theory for the simpler metals. Here we try to crudely model kinetic energy effects in such a way as to approximate their properties in any correct band theory calculation.

In these cases we may deal exclusively with the energies of the valence electrons in Eqs. (4) and (5), and it is convenient to introduce another logarithmic parameter λ_v which may be used to evaluate τ_v for the valence electrons

$$\lambda_v \equiv \frac{d\ell nt_v}{d\ell n\rho} \ , \ \tau_v = \lambda_v + \frac{d\ell n\lambda_v}{d\ell n\rho} \qquad (12)$$

First we try an estimate of the enhancement of τ_v by a simple, one-dimensional gas model for radial kinetic energies in which electrons are confined between the Wigner-Seitz and inner core radii of R and R_c where

$$R_c = K_c R \ . \qquad (13)$$

Then for instance λ_v of Eq. (11) is the sum of distortional variations of the kinetic energy $t(K_c,R)$ with respect to K_c and scaling variations with respect to R. Table 3 shows calculations of the resulting increase, of λ_v and τ_v with the ratio K_c.

Table 3. Core size dependence of kinetic energy for square well model

K_c	1/4	1/3	1/2	2/3
λ_v	8/9	1	4/3	2
τ_v	1	7/6	5/3	8/3
$d\tau_v/d\ell n\rho$	.15	.25	.67	(2)
$d^2\tau_v/d(\ell n\rho)^2$	.08	.17	.67	(2.3)

The large values of the higher derivatives at the largest K_c are taken to be upper limits due to model deficiencies.

The second non-perturbative model for valence energy changes we have used is a semiclassical calculation of low ℓ-band eigenstates in the Thomas-Fermi potential, v_{TF}. Radial eigen-values, and the corresponding kinetic energies, t_ℓ, can be simply calculated from the semi-classical phase integral and the corresponding density of states integral, $n_{\ell\varepsilon}$,

$$t_\ell \propto 1/n_{\ell\varepsilon} ,$$

$$n_{\ell\varepsilon} = \frac{1}{\pi}\int_{-}^{+} \frac{dr}{k} , \quad k \equiv \sqrt{2(\varepsilon - v_{TF})} . \tag{14}$$

Estimating derivatives numerically we have obtained the results in Table 4 for λ in low band states for cases where both centrifugal potential (p-states in C) core orthogonalization (s-states in Rb) are operative.

Table 4. Semiclassical calculations of τ in Thomas-Fermi potential

Element	$Z^{1/3}R_o$	τ_{TF}	K_c	λ_o	λ_1
C	3.82	> 1	~.2		~1.0
Rb	18.0	~.6	~.25	~1.7	--

λ varies slowly with R in these calculations so that we may compare λ directly with τ_{TF}, from Table 2. Large values of λ are seen to occur in the cases of orthogonalization cores. These larger values as well as the even larger values from complete band structure calculations can average out to the lower TF values by transfer of electrons to higher angular momentum states with compression as required by the TF model. This mechanism plays a key role also for certain structural phase transitions of the solid elements, as reviewed by McMahan.[4]

λ values in Table 4 are particularly large in view of listed values of calculated core radii and the square well results of Table 3. This appears to be due to the kinetic energy changes in the valence state itself which are occurring in the outer part of its wave function. This is the result of local variations in the electron kinetic energy changes being proportional to 1/k [see Eq. (14)]. Thus the square-well model value of K_c should refer to a larger value, which partitions the valence potential between regions of weak and strong values which occur only under core orthogonalization conditions.

REFERENCES

1. R. Jeanloz and R. Grover (previous article this volume).

2. R. Grover, Birch Expansions Beyond 2-Fold Compression, Lawrence Livermore Nat. Lab. UCRL-95388 (1986).

3. A.L. Ruoff, J. Applied Phys. 38 (1967) 4976
S.P. Singh, Phys. Rev. B, 9 (1973) 3313
K-J. Dunn, Phys. Rev. B, 12 (1975) 3497

4. A.K. McMahan, Physica 139 & 140 B (1986) 31.

5. D.J. Steinberg, J. Phys. Chem. Solids 43 (1982) 1173.

6. Note the smallness of A_2 and A_3 in Table 1 arise from Eq. (7), requiring that roots of A_2 be 11/3 and 13/3 and Eq. (8), that A_3's roots are $(11 \pm \sqrt{3})/3$ and 16/3!